

DOE/NASA/1040-18
NASA TM-81578

Evaluation of Candidate Stirling Engine Heater Tube Alloys for 1000 Hours at 760° C

John A. Misencik
National Aeronautics and Space Administration
Lewis Research Center
Cleveland, Ohio 44135

November 1980

Work performed for
U.S. DEPARTMENT OF ENERGY
Conservation and Solar Energy
Office of Transportation Programs
Washington, D.C. 20545
Under Interagency Agreement EC-77-A-31-1040

Summary

Six tubing alloys were endurance tested in a diesel-fired, Stirling engine simulator materials test rig for 1000 hours at 760° C while pressurized at 17 to 21 MPa with either hydrogen or helium. The alloys tested were N-155, A-286, Incoloy 800, 19-9DL, Nitronic 40, and 316 stainless steel. All alloys were in the form of tubing with an outside diameter of 4.8 mm and a wall thickness of 0.8 mm. Hydrogen permeated rapidly through the walls of all six alloys when they were heated to 760° C, and repressurization was required every 5 hours during rig testing. In contrast, helium was readily contained. Creep-rupture failures occurred in four of the six alloys pressurized with helium and in two of the six alloys pressurized with hydrogen. Only two alloys survived the 1000-hour endurance test with no failure, N-155 and 316 stainless steel. Simultaneous exposure to either hydrogen or helium and the combustion environment at 21 MPa and 760° C did not seriously degrade the tensile strength of the six alloys in tests at room temperature and 760° C after exposure. Decreases in room-temperature ductility were noted and are attributed to aging rather than to hydrogen embrittlement or oxidation in three of the alloys. However, there may be a hydrogen embrittlement effect in the N-155, 19-9DL, and Nitronic 40 alloys.

Introduction

The work described in this report was conducted as a part of the supporting research and technology activities under the DOE-NASA Stirling Engine Highway Vehicle Systems program (ref. 1).

In the Stirling engine for automotive application the working fluid, hydrogen, is passed through the hot zone in a series of small thin-wall tubes, which are required for efficient heat transfer from the hot zone to the working fluid (ref. 2). The hot, high-pressure gas is then expanded to drive one or more pistons, which actuate the drive system. After cooling, the gas is then recirculated back to the hot zone to repeat the cycle. Containment of hydrogen in the high-temperature heater tube assembly is essential for proper performance. In addition, materials reliability under the influence of this high-pressure hydrogen (21 MPa) at high temperature (760° to 870° C) must be assured. To meet these requirements, an iron-base superalloy (N-155) is

presently being used for heater tubes in the high-temperature heating assembly. As this alloy contains approximately 20 percent cobalt, which is expensive and in short supply, alternative materials are desirable (ref. 3). Thus a major long-term goal of the materials technology program is to identify or develop a strong, oxidation-resistant, low-cost alloy for this application.

The work described in this report was conducted to evaluate the performance of N-155 and five other candidate heater tube alloys under conditions of temperature, pressure, and environment (hydrogen and combustion products) that simulate the actual operation of a Stirling-powered highway vehicle. The other candidate alloys were A-286, Incoloy 800, 19-9DL, Nitronic 40, and 316 stainless steel. The data presented are from the first 1000-hour endurance test conducted in the NASA Lewis Stirling engine simulator test rig.

Experimental Procedures

Materials

The six alloys used in this study were obtained commercially in the form of tubing with an outside diameter of 4.8 mm and an inside diameter of 3.2 mm. Three of the alloy tubes were weld drawn: N-155, 19-9DL, and Nitronic 40; and three were seamless: A-286, Incoloy 800, and 316 stainless steel.

Chemical analyses of the six alloys as reported by the fabricator are shown in table I. All are iron-base superalloys with substantial amounts of nickel and chromium. Note that Nitronic 40 has 9.0 percent manganese substituted for some of the nickel. Average grain sizes ranged from 9 μm for 19-9DL to 32 μm for Incoloy 800. The microstructures of the six alloys in the as-received condition are shown in figure 1.

The tubing alloys were evaluated in the Stirling materials rig in the form of hairpins, as shown in figure 2. Each leg of the hairpin was 30.5 cm long with 2.5 cm between legs. Four of these hairpin tubes were attached to a copper module with internal passages and external tubes and valves for filling each module with the proper gas (hydrogen or helium). A module with hairpin tubes attached is shown in figure 3. The tubing was attached to the module with gas-tight mechanical connectors. Also shown in figure 3 is the thermocouple that was

attached at the bottom of the hairpin tube and the lead to the pressure transducer that was located adjacent to the thermocouple plug at the top of the module. The hairpin tubes were connected in series and were filled through the tubing and valves located on top of each module. When one tube failed, the pressure in the remaining three was lost.

Before installation in the rig each assembled module was leak checked to 10 MPa with helium by submersion under water and then proof tested to 30 MPa with Varsol (an organic liquid). The module was then flushed with acetone. The proof pressure of 30 MPa is three times the room-temperature charging pressure of 10 MPa and 1.5 times the maximum pressure at the operating temperature of 760° C. Little difficulty was experienced in achieving leakproof modules, and no failures were experienced during proof testing of the 12 modules. "High purity" hydrogen (commercially procured) was used during the first 500 hours of rig testing. Analyses of the hydrogen are shown in table II. Note that the oxygen content of high-purity hydrogen averaged 53 ppm. Commercial-purity hydrogen was used during the last 500 hours of rig testing in order to evaluate purity effects on hydrogen retention. The oxygen content of this hydrogen ranged from 364 to 526 ppm for all bottles except one, where oxygen was not detected. Individual bottles of commercial-purity hydrogen contained 1.32-vol% CO, 23.2 ppm H₂O, or 157 ppm CH₄. Analyses of the helium used revealed no detectable amount of oxygen.

Stirling Simulator Rig

The Stirling simulator test rig used in this program was designed and fabricated at the Lewis Research Center; it consists primarily of a heating chamber with an auxiliary heating, control, and gas-management system. A schematic of the heating chamber is shown in figure 4. The heating chamber consists of a doubled-walled, air-cooled, closed cylinder with a combination diesel oil and natural gas burner at the bottom. An air blower supplies combustion air to the burner and cooling air to the chamber walls and the burner. A thin layer, 1.3 cm, of insulation between the double walls of the chamber and a 7.6-cm layer at the top aid in keeping the outside of the heating chamber cool. The combustion gases are vented outside the building through a 25-cm doubled-walled exhaust stack. Two of these rigs have been constructed and are shown in figure 5.

The heating chamber is fitted with two thermocouples, one for temperature control and a second for overtemperature automatic shutdown. The burner control includes two timers for automatic

cycling; thus, two heating cycles of different durations can be run either once or in multiple series. To permit automatic unattended operation, the supply systems for air, oil, natural gas, and cooling water are all equipped with safety pressure sensors and automatic shutoff valves. If any of these delivery systems should fail, the entire rig is automatically shut down. The 1000-hour endurance test was not conducted in the automatic mode but rather in 5-hour cycles that were manually started and automatically shut down. This mode of operation was necessitated by the requirement for hydrogen repressurization after each cycle.

Each rig has 12 test modules located at the top of the heating chamber (fig. 4). These modules are installed by insertion into holes spaced around the top of the heating chamber. Each module is bolted to the top of the heating chamber. Each is equipped with a pressure transducer with a range from 0 to 34 MPa. These transducers are strain-gage devices made of 304 stainless steel and sealed to the module with an elastomeric "O" ring. Cooling of the modules near the transducer was achieved by situating the modules on water-cooled copper blocks. Each module was also equipped with a Chromel-Alumel thermocouple wired to the bottom of one of the hairpins. This can be seen in figure 3. The temperature and pressure from each module were continuously recorded during rig operation.

Each rig is equipped with helium or hydrogen charging manifolds located on the top cover of each heating chamber, as shown in figure 6. These manifolds and the two valves on each module permit evacuation and charging of the modules. The modules are arranged around the top of the rig such that alternate modules contain the same gas (hydrogen or helium). Thus six modules (one of each alloy) were charged with hydrogen and six with helium during the 1000-hour endurance run. The modules containing a given gas could be charged individually or as a group. Standard charging procedure consisted of evacuation to 10⁻⁵ MPa and flushing with helium. After the third flush the modules that were to contain helium were pressurized to 10 MPa. The modules that were to be filled with hydrogen were purged with hydrogen for 15 seconds and then pressurized to 10 MPa.

A typical heating cycle consisted of a 1.5-minute preheat with natural gas, a 2-minute burn with a combination of natural gas and low-pressure diesel oil, a 1.5-minute burn with a combination of natural gas and high-pressure diesel oil, and a 5-hour burn with high-pressure diesel oil. A 2-minute gas burn was used at the end of each 5-hour cycle. The cooldown time between cycles was 1 hour or longer. After cooldown the modules containing hydrogen were vented and refilled. The helium modules did not

require refilling after each cycle; they were evacuated and refilled only after hairpin replacement following failure or leak. The helium pressure was maintained at 17 to 21 MPa during the 5-hour cycles until two hairpins of a given module failed. After this the pressure in that module was reduced to 1 to 2 MPa to prevent further hairpin failures and to allow post-test mechanical property comparison with the hydrogen-containing tubes, which usually did not fail during the 1000-hour test run. After completion of the test run or after failure, the hairpins were removed from the modules and sectioned for testing.

The temperature profile inside the heating chamber of the rig was determined at the start of the 1000-hour endurance run. The profile was determined by measuring the temperature at three locations on each module. The thermocouples were fastened to each module at the bottom bend of the hairpin, 10.2 cm from the bottom bend, and 22.9 cm from the bottom bend.

Postexposure Evaluations

Postexposure evaluation included both tensile testing and metallography.

Tensile tests were conducted on tube specimens at room temperature and at 760° C. The grips and a tensile specimen are shown in figure 7. The bottom of the tensile specimen is enclosed in the grips. An exploded view of the grip components is shown at the top of the specimen. The specimens were 10.2 cm long for testing at room temperature and 17.8 cm long for testing at 760° C. A solid tool steel pin 2.5 cm long was inserted into the tube ends to prevent collapse of the tube during testing. The elongation after testing was determined from measurements on prescribed marks on the tensile specimens. All tests were conducted at a crosshead speed of 0.25 cm/sec.

The metallographic specimens were sectioned from a hairpin tube taken from each module. The specimens were polished, etched, and then examined at magnifications of 100X and 500X.

Results

Temperature Profile

The results of the temperature profile run are shown in figure 8. This figure shows the temperature at the top, middle, and bottom locations on the module plotted against the angular position around the furnace. At the top location the temperature varied from 746° C to 798° C, with the highest temperature at the 30° (module 1) location. The

temperature at the middle location varied from 740° C to 760° C. The greatest temperature variation was at the bottom location, where the temperature varied from 730° C at the 90° (module 3) location to 780° C at the 60° (module 2) location. The 90° location is the position of a sight port through which a small amount of additional cooling air enters the hot zone. This was probably the cause of the lower temperature at this location.

Pressure-Time Relationships

Hydrogen pressure-time data for all six alloys for five selected cycles during the 1000-hour endurance test are presented in table III. The cycles selected were 9, 49, 101, 153, and 202. These represent 45, 250, 500, 750, and 1000 hours, respectively, of the endurance test. The data show a rapid rise in pressure, to 17 to 21 MPa usually within 10 minutes, and then a decay in pressure during the remainder of the cycle. This pressure decay with time results from permeation of hydrogen through the hot tube walls and varied with the alloy, with the impurity content of the hydrogen, and with time during the endurance run.

Examination of the data in table III shows that large changes in the pressure decay characteristics occurred in N-155, Incoloy 800, Nitronic 40, and 316 stainless steel. Little or no change took place in A-286 and 19-9DL. The greatest changes occurred in Incoloy 800 and Nitronic 40 during the last half of the endurance test, represented by cycles 153 and 202. Typical pressure decay curves for Incoloy 800 are shown in figure 9.

Under conditions such that the diffusion of hydrogen through the metal lattice is rate controlling, the permeation flux is described by

$$j = \frac{dV}{dt} = \varphi \frac{A}{l} (P_1^{1/2} - P_2^{1/2}) \quad (1)$$

where

- j flux, cm³/sec
- V volume, cm³
- t time, sec
- φ permeability coefficient, cm²/sec MPa^{1/2}
- A permeating area, cm²
- l membrane thickness, cm
- P_1 gas pressure on entrance side of membrane, MPa
- P_2 gas pressure on exit side of membrane, MPa

For a closed system the pressure P as a function of time t can be calculated by rearranging and integrating equation (1) to give

$$P^{1/2} = P_0^{1/2} - \frac{\varphi A P_s T_1 t}{2 V_1 T_s} \quad (2)$$

where

P pressure in closed system, MPa
 P_0 original pressure, MPa
 P_s standard pressure, MPa
 T_1 temperature of system, K
 V_1 volume of system, cm³
 T_s standard temperature, K

This relationship strictly applies to a flat sheet specimen; however, it is suitable for the calculation of approximate permeability coefficients for the tube specimens. The permeability coefficient φ was calculated for each alloy, with the results shown in table IV. The permeability coefficient φ varied from 1.1×10^{-5} for 316 stainless steel during cycle 9 to 3.3×10^{-7} for Nitronic 40 during cycle 153. Also shown in table IV are the average permeability coefficients for the first 500 hours (cycles 9, 49, and 101), during which high-purity hydrogen was used. In all cases the average permeability coefficients for the first 500 hours into the endurance run were greater than those for the last 500 hours, where commercial hydrogen was used. The largest changes in the average permeability coefficient were for Incoloy 800 and Nitronic 40, with smaller changes in N-155 and 316 stainless steel. Little change was noted for A-286 and 19-9DL.

The permeability coefficients for four of the alloys (N-155, A-286, Incoloy 800, and 19-9DL) obtained during the first 500 hours are compared in the following table with those obtained for the same four alloys at 760° C in another program (ref. 4) in which very high-purity hydrogen with less than 1 ppm oxygen was used:

	This study	Reference 4
	Permeability coefficient, cm ² /sec MPa ^{1/2}	
N-155	7.0×10^{-6}	1.8×10^{-5}
A-286	5.2	1.5
Incoloy 800	3.6	1.4
19-9DL	5.8	1.4

Note that the permeability coefficients for the four alloys in each study are all of the same order of magnitude and that the differences between the two studies are within a factor of 4, with the higher permeabilities occurring in the study with the higher purity hydrogen.

A factor that is considered to have a large influence on apparent permeability rates is the condition of the surface of the metal. In particular, the presence or absence of a surface oxide film should have a large influence on the apparent permeability of the hydrogen through the tube wall. Examination of the data in table IV indicates that the increased oxygen content of the hydrogen used after 500 hours can be correlated with reduced hydrogen permeability during subsequent cycles. The large changes in permeability for Incoloy 800 and Nitronic 40 are postulated to be due to the formation of oxide films on the inside surface of the tube since there are several highly stable oxide formers in these two alloys. These oxide formers are chromium, manganese, titanium, silicon, and aluminum.

To determine if any oxide layers were present on the inside surface of the tubes, cross sections of the exposed tubes were examined metallographically and by X-ray diffraction. Figure 10 shows the cross sections for each alloy at a magnification of 100X. Figure 11 shows a typical inside surface of a tube at 500X. No oxide layer could be identified on any of the inside surfaces at a magnification of 500X. However, X-ray diffraction studies made on particles scraped from the inside surfaces of the tubes identified trace amounts of sesquioxides (Fe₂O₃-Cr₂O₃). This identification was made with difficulty since the amount of oxide on the inside of the tubes was very small.

The inner edge of the Nitronic 40 tube that was exposed to hydrogen is shown in figure 12. A reaction has taken place on the inner edge to a depth of approximately 0.06 mm. The Nitronic 40 tube that was exposed to helium for 542 hours did not show this effect. The nature of this reaction has not yet been identified.

Metallographic examination of the outside surfaces of the tubes revealed a thick oxide layer on several outside surfaces. Figure 13 shows the thick layer present on the 19-9DL and 316 stainless-steel tubes. This layer has also been identified as a sesquioxide (Fe₂O₃-Cr₂O₃).

One consequence of the loss of hydrogen through the hot walls of the heater tubing in a Stirling engine is the requirement to recharge the system with hydrogen in order to maintain engine power. We estimate that a 10 percent loss in hydrogen would require a recharge. It would be desirable to recharge no more frequently than once every 6 months, equivalent to about 170 hours of actual driving time. Using the permeability coefficients for the six alloys and assuming commercial-purity hydrogen, a 7-liter reservoir at 21 MPa, and a 1-liter engine capacity at 720° C, we estimate the time required between recharging operations (10 percent hydrogen loss) as follows:

	Recharging interval, hr
N-155	70
A-286	50
Incoloy 800	370
19-9DL	40
Nitronic 40	230
316 Stainless steel	100

Only two alloys, Incoloy 800 and Nitronic 40, would require less frequent recharging than the desired 6-month time period. The calculated times between engine recharges with hydrogen should be treated only as estimates. They also will vary with reservoir size and with pressure.

Tubing Failures

Many of the hairpin tubes failed during the 1000-hour endurance test. The tubes that contained helium experienced more failures than did those that contained hydrogen because of the constant pressure maintained in the helium-containing tubes throughout each of the 5-hour cycles. In contrast, the hydrogen pressure decayed with time and thereby reduced the stress in the tube wall for part of each cycle. The tube failure times are shown in table V.

Tubing failures occurred in four of the six alloys that contained helium. One tube of A-286 failed at 710 hours, one tube of Incoloy 800 failed at 614 hours, and six tubes of 19-9DL failed at 164 to 273 hours. Six tubes of Nitronic 40 failed during the endurance test at times ranging from 120 to 192 hours. No tubing failures occurred in the N-155 or 316 stainless-steel alloys.

In those modules that contained hydrogen, only two experienced failures. These were 19-9DL at 820 to 973 hours and Nitronic 40 at 163 to 619 hours. These two alloys also had the most failures in those tubes that contained helium.

Tensile Properties

The tensile properties of the as-received tubing were determined at NASA Lewis. After completion of the 1000-hour endurance test, the hairpin tubes of the six alloys were sectioned for tensile testing to determine the effect of rig environment on tensile properties. Each of the six alloys had been exposed to both hydrogen and helium in addition to the burner combustion products at 760° C for 1000 hours. Both room-temperature and high-temperature (760° C) tensile tests were conducted. Two specimens of each alloy were tested at room temperature, and at least one specimen representative of each alloy and environment was tested at 760° C. The results of

these tests are described in the following sections.

As-received properties.—The room-temperature tensile properties of the as-received tubing are presented in table VI. The ultimate strengths of the six alloys ranged from 878 MPa for N-155 to 600 MPa for Incoloy 800. The three highest strength alloys were N-155, 19-9DL, and Nitronic 40. The tensile elongations were good for all six alloys, ranging from 34.5 percent for A-286 to 54 percent for 316 stainless steel.

The high-temperature tensile properties of the as-received materials are given in table VII. The tensile strengths at 760° C ranged from 434 MPa for A-286 to 226 MPa for 316 stainless steel. The tensile elongations ranged from 56 percent for Incoloy 800 to 26.5 percent for 19-9DL.

Post-endurance-test properties.—The tensile data at room temperature and at 760° C for the six alloys after exposure under pressure with hydrogen and helium in the rig for 1000 hours are given in tables VI and VII, respectively. Exposure in the rig resulted in little or no reductions in tensile strength at room temperature for all six alloys studied. Two alloys, A-286 and 316 stainless steel, showed higher strengths after exposure. There were, however, large reductions in ductility for three of the alloys—N-155, A-286 and 316 stainless steel—after exposure during the 1000-hour endurance test. In these three alloys, both the tubes that contained hydrogen and those that contained helium were affected, an indication that aging embrittlement had occurred. The large reduction in ductility for N-155 suggests hydrogen embrittlement in this alloy. This may also be true for 19-9DL and Nitronic 40 since both alloys showed slight reductions in ductility in those tubes that contained hydrogen. Note, however, that none of the tubes of these two alloys survived the 1000-hour endurance test and that the tubes that contained hydrogen were exposed longer in the rig than those that contained helium. The losses in ductility in 19-9DL and Nitronic 40 alloy tubes that contained hydrogen may be an aging effect caused by the longer times at temperature.

Comparisons of the 760° C tensile data show that N-155, A-286, and 19-9DL were weakened by exposure at 760° C for 1000 hours. The reductions in ultimate strength occurred in both the tubes that contained hydrogen and those that contained helium, an indication of an aging reaction.

Discussion

The results of the first 1000-hour endurance test at 760° C indicate that the Stirling engine simulator materials test rig is a useful tool for evaluating heater tube alloys. The ability to test several alloys under

two different gaseous environments at various pressures is a distinct advantage over on-the-road vehicle testing, test cell engine testing, or static laboratory materials tests. The temperature variation of 68 degrees at 760° C in the heating chamber, although large for laboratory creep-rupture testing, is adequate for determining high-temperature material behavior trends and for approximating permeability in heater tubes. It has been shown that helium can readily be contained in the heater tubes at 21 MPa and 760° C but that hydrogen permeates through the tube walls and must be replenished periodically. The use of helium in Stirling engines is technically feasible; however, the loss in engine efficiency due to the higher molecular weight of helium is a powerful driver for the use of hydrogen (ref. 5).

During the early 5-hour segments of the endurance test all alloys lost hydrogen rapidly. The inability to maintain a constant hydrogen pressure throughout a 5-hour cycle is a deficiency of the rig; however, approximations of hydrogen permeability were determined for each of the alloys. The hydrogen loss rate was greater during the first half of the 1000-hour endurance run, where high-purity hydrogen was used, than during the last half, where commercial-purity hydrogen was used. The major difference between these two types of hydrogen is the presence of approximately 350 ppm of oxygen in commercial-purity hydrogen. This small amount of oxygen decreased hydrogen permeability in all alloys. There were substantial decreases in hydrogen permeability in Incoloy 800 and Nitronic 40 and lesser decreases in N-155 and 316 stainless steel. These reduced permeabilities during the later segments of the endurance run are thought to be associated with the formation of very thin oxide films on the inside surfaces of the tubes. Thus the presence of strong oxide formers such as chromium, manganese, titanium, silicon, and aluminum in the alloy in conjunction with the oxygen impurity appear necessary for reducing hydrogen permeability. No attempts were made to use hydrogen with larger additions of oxygen because mixtures with as little as 4 percent oxygen are explosive.

The permeability coefficients for the six alloys were used to estimate the time required to effect a 10 percent hydrogen loss in a Stirling engine with a hydrogen reservoir. This estimate was made for a 1-liter engine and a 7-liter reservoir. The results show that two of the alloys would contain hydrogen adequately for 6 months or longer of normal driving. These alloys were Incoloy 800 and Nitronic 40. The times calculated for recharging the engine with hydrogen should be treated only as estimates since conditions inside the Stirling engine are different

from those in the rig. One such difference is that oil required in the Stirling engine can and apparently does contaminate the hydrogen during engine operation. This oil contamination can result in carbide formation in addition to oxide surface films being deposited on the tube walls, thereby reducing the rate of hydrogen loss from the engine (ref. 6).

The room-temperature tensile properties of the alloys were not severely degraded by the 1000-hour exposure with hydrogen or helium. The tensile strengths of A-286 and 316 stainless steel were slightly higher after the endurance test than in the as-received condition, and there was a slight loss in room-temperature elongation for these two alloys and for N-155. When they were tested at 760° C after the 1000-hour exposure, the tensile strengths of N-155, A-286, and 19-9DL were lower than in the as-received condition. The reductions in strength were not large, and there were no large differences in microstructure between the as-received and exposed tubing.

Sheet specimens of the six alloys in the as-received condition have been evaluated in creep rupture in another part of the Stirling materials evaluation program (ref. 7). The results are shown in table VIII. Based on a hoop stress of 50.5 MPa (calculated for a gas pressure of 19.3 MPa), the rupture lives predicted from the creep-rupture study varied from greater than 60 000 hours for the N-155 to 350 hours for 316 stainless steel. The average lives of the helium-filled tubes during the endurance run, as shown in table VIII, varied from 154 hours for Nitronic 40 to greater than 1000 hours for N-155 and 316 stainless steel. In general, the results of the creep-rupture tests were consistent with the order of failure of the alloys in the rig, except for 316 stainless steel. The creep-rupture study indicated this to be the weakest alloy, but no failures occurred during the 1000-hour endurance test. Furthermore the creep-rupture lives were greater than those observed during rig testing. These differences may be due to different methods of manufacture for the sheet and tubing specimens, temperature variations in the rig, or slight chemistry differences between the sheet and tubing specimens. In addition, the grain size of the material has a marked effect on rupture strength of these alloys. For example, it was shown for 19-9DL (ref. 7) that increasing the grain size from 5 μm to about 28 μm produced a concomitant increase in rupture strength of a factor of 4 over the temperature range 700° to 815° C. The relatively fine grain size of 9 μm for the 19-9DL tubing used herein probably attributed to its relatively short life in the Stirling materials rig. We estimate that a life of at least 1000 hours in the rig test would be required for consideration of an alloy for the engine application.

In view of the failures that occurred during the 1000-hour endurance test and the rapid loss of hydrogen during each of the 5-hour cycles, especially when pure hydrogen was used, none of these heater tube candidate alloys possesses both adequate strength and adequate resistance to hydrogen permeability at 760° C. To obtain a low-cost heater tube alloy, it appears that alloy modification will be necessary to provide the combination of high strength and low permeability required.

Summary of Results

Endurance testing of six tubing alloys in a diesel-fired Stirling engine simulator materials test rig for 1000 hours at 760° C and 17 to 21 MPa had the following results:

1. All alloys lost hydrogen rapidly during the early 5-hour segments of the endurance test, when high-purity hydrogen was used. Loss rates for Incoloy 800 and Nitronic 40 decreased significantly during the last 500 hours of the test, when commercial-purity hydrogen was used.

2. Permeability of hydrogen through the alloy tubing is strongly affected by the alloy composition and the oxygen content of the hydrogen. Oxygen contents as low as 350 ppm substantially reduced the permeability in Incoloy 800 and Nitronic 40. Lesser reductions in permeability were also observed for N-155 and 316 stainless steel.

3. The reduced permeabilities during the later segments of the endurance tests are thought to be associated with formation of thin oxide films on the inside surfaces of the tubes. It is further postulated that these films require the presence of strong oxide formers such as chromium, manganese, titanium, silicon, or aluminum in the alloy plus oxygen as an impurity in the hydrogen.

4. Tensile strengths at room temperature were increased for A-286 and 316 stainless steel, but the strengths of the other four alloys were hardly affected by the 1000-hour exposure to hydrogen or helium. The loss in room-temperature ductility for N-155 indicates a possible hydrogen embrittlement effect.

5. Tensile strengths at 760° C were reduced after endurance testing for N-155, A-286, and 19-9DL. The strengths of the other three alloys were essentially unaffected. Tensile elongations of all alloys evaluated were above 20 percent after endurance testing.

6. Creep-rupture failures in tubes pressurized with helium occurred with four of the six alloys tested. No failures occurred in N-155 and 316 stainless steel. The failure times could generally be correlated with expected creep-rupture life.

References

1. Brogan, J.J.: Highway Vehicle Systems Program Overview. Highway Vehicle Systems, CONF-771037, 1978, pp. 3-5.
2. Walker, G.: Stirling Cycle Machines. Clarendon Press, Oxford, 1973.
3. Stephens, J.R.; et al.: Materials Technology Assessment for Stirling Engines. NASA TM-73789, 1977.
4. Vesely, E.J., Jr.: Hydrogen Permeability in Uncoated and Coated Metals. Highway Vehicle Systems, CONF-791082, 1979, pp. 86-98.
5. Cairelli, J.E.: Initial Test Results with Single Cylinder Rhombic Drive Stirling Engine. Highway Vehicle Systems, CONF-771037, 1978, pp. 254-258.
6. Stephens, J.R.: Stirling Materials Development. Highway Vehicle Systems, CONF-7904105, 1979, pp. 262-272.
7. Witzke, W.R.; and Stephens, J.R.: Creep-Rupture Behavior of Seven Iron-Base Alloys After Long Term Aging at 760° C in Low Pressure Hydrogen. NASA TM-81534, 1980.

TABLE I. - COMPOSITION OF TUBING ALLOYS

Alloy	Heat	Fabrication	Grain size, μm	Element														
				Cr	Ni	Co	Mn	Mo	W	Ti	Nb	Si	Al	C	N	Cu	V	Fe
				Composition, wt% ^a														
N-155	C102770	Weld drawn	17	21.2	19.9	19.0	1.45	3.03	2.61	----	1.05	0.55	----	0.11	0.16	----	----	Bal.
A-286	27771	Seamless	11	14.4	24.7	----	1.01	1.17	----	2.12	----	.62	----	.06	----	0.32	0.26	-----
Incoloy 800	HH6127A	Seamless	32	22.5	32.6	----	.73	----	----	.52	----	.53	0.54	.01	----	.03	----	-----
19-9DL	C35039	Weld drawn	9	18.3	8.76	----	1.02	1.26	1.18	.27	^b .37	.47	----	.29	----	----	----	-----
Nitronic 40	800128	Weld drawn	15	20.8	7.02	.09	9.36	.03	----	----	----	.49	----	.03	.34	----	----	-----
316 Stainless steel	07475	Seamless	21	17.3	13.1	----	1.57	2.26	----	----	----	.54	----	.06	----	----	----	-----

^aVendor analyses.^bCb/Ta.

TABLE II. - HYDROGEN ANALYSES FOR 1000-HOUR

ENDURANCE TEST AT 760° C IN RIG A

Cycle	Test time, hr	Hydrogen type	Nitrogen	Oxygen	Argon	Carbon dioxide	Other
			Composition, ppm ^a				
66	^b 330	High purity	3605	43	23	90	-----
78	372	<div style="text-align: center;"> ↓ Commercial purity </div>	4425	43	0	39	-----
90	437		3862	65	0	206	-----
104	511		3329	61	0	73	-----
113	552		1576	431	13	141	1.32 vol.% CO
124	611		2624	364	25	221	-----
135	658		3251	386	0	595	-----
148	728		1050	526	25	152	23.4 Water
163	804		2346	415	24	121	-----
174	856		2525	438	24	122	-----
185	912		3782	0	0	178	-----
199	982		2793	502	13	143	157 Methane

^a Except where noted.^b No analyses before 330 hr - all high purity.

TABLE III. - HYDROGEN PRESSURE DECAY FOR FIVE SELECTED CYCLES
DURING 1000-HOUR ENDURANCE TEST

(a) N-155

Cycle									
9		49		101		153		203	
Cycle time, min	Pressure, MPa	Cycle time, min	Pressure, MPa	Cycle time, min	Pressure, MPa	Cycle time, min	Pressure, MPa	Cycle time, min	Pressure, MPa
10	19.0	8	19.1	8	20.3	10	18.1	11	18.4
24	17.2	22	17.2	33	17.2	25	17.2	38	17.2
60	13.0	60	11.7	60	14.5	60	15.0	60	16.2
120	7.6	120	5.5	120	9.2	120	11.7	120	13.6
180	3.9	180	2.1	180	5.5	180	9.6	180	11.6
240	1.9	240	.3	240	3.0	240	7.2	240	9.8
300	.8	300	.1	300	1.6	300	5.3	300	8.1

(b) A-286

10	19.0	8	19.0	8	20.5	10	17.8	11	18.3
34	17.2	25	17.2	37	17.2	19	17.2	27	17.2
60	15.0	60	13.1	60	15.2	60	14.1	60	15.0
120	10.8	120	7.8	120	10.5	120	10.5	120	11.6
180	7.8	180	4.6	180	7.2	180	7.8	180	8.8
240	5.4	240	2.2	240	4.8	240	5.4	240	6.7
300	3.9	300	1.0	300	3.3	300	4.0	300	5.2

(c) Incoloy 800

10	19.6	8	20.3	7	20.9	10	18.8	15	19.3
38	17.2	55	17.2	---	---	---	---	---	---
60	15.0	60	16.9	75	17.2	60	18.1	60	19.1
120	10.0	120	13.2	120	15.2	120	17.2	120	18.8
180	6.6	180	10.3	180	12.8	180	16.4	180	18.3
240	4.3	240	8.0	240	10.7	240	15.6	240	17.8
300	2.9	300	6.0	300	9.1	300	14.8	300	17.2

TABLE III. - Concluded.

(d) 19-9DL

Cycle									
9		49		101		153		203	
Cycle time, min	Pressure, MPa	Cycle time, min	Pressure, MPa	Cycle time, min	Pressure, MPa	Cycle time, min	Pressure, MPa	Cycle time, min	Pressure, MPa
10	19.3	8	19.6	8	20.5	10	18.4	12	17.9
37	17.2	34	17.2	37	17.2	22	17.2	21	17.2
60	15.0	60	15.1	60	15.0	60	13.8	60	13.3
120	10.3	120	9.3	120	9.1	120	9.5	120	8.4
180	6.9	180	5.7	180	5.3	180	6.4	180	5.0
240	4.4	240	3.3	240	2.9	240	4.1	240	2.8
300	2.9	300	1.8	300	1.6	300	2.6	300	1.7

(e) Nitronic 40

12	19.3	8	20.3	10	20.7	38	20.0	15	18.4
35	17.2	38	17.2	39	17.2	---	---	---	---
60	15.6	60	15.6	60	15.0	60	19.9	60	17.9
120	12.1	120	9.5	120	9.3	120	19.5	120	16.4
180	9.1	180	5.9	180	5.7	180	19.2	180	14.8
240	6.9	240	3.6	240	3.2	240	18.8	240	13.4
300	5.3	300	2.1	300	1.7	300	18.3	300	12.2

(f) 316 Stainless steel

10	19.0	8	19.6	10	20.7	10	18.6	15	18.8
20	17.3	28	17.2	54	17.2	50	17.2	---	---
60	10.0	60	13.2	60	16.9	60	16.9	62	17.2
120	3.0	120	7.2	120	12.4	120	14.6	120	15.0
180	.3	180	3.4	180	9.1	180	12.6	180	12.9
240	.2	240	1.4	240	6.4	240	10.8	240	11.2
300	.2	300	.5	300	4.3	300	9.1	300	9.5

TABLE IV. - HYDROGEN PERMEABILITY COEFFICIENTS AT 760° C

Alloy cycle	Alloy					
	N-155	A-286	Incoloy 800	19-9DL	Nitronic 40	316 Stainless steel
	Permeability coefficient, $\text{cm}^2/\text{sec MPa}^{1/2}$					
9	6.6×10^{-6}	4.3×10^{-6}	5.3×10^{-6}	5.0×10^{-6}	4.0×10^{-6}	11.0×10^{-6}
49	8.6	6.6	3.3	5.7	5.8	7.2
101	5.9	4.8	2.3	6.6	6.0	4.0
153	3.2	4.0	.74	4.8	.33	2.0
202	2.3	3.5	.38	5.6	1.2	2.0
Average for 9, 49, 101	7.0	5.2	3.6	5.8	5.3	7.4
Average for 153, 202	2.8	3.8	.56	5.2	.78	2.0

TABLE V. - TUBING FAILURE TIMES DURING
760° C ENDURANCE TEST

Alloy	Failure times, hr in indicated environment	
	Helium	Hydrogen
N-155	(a)	(a)
A-286	710	(a)
Incoloy 800	614	(a)
19-9DL	164	820
	203	901
	217	973
	263	(a)
	269	(a)
Nitronic 40	276	(a)
	120	163
	131	226
	143	600
	164	619
	175	(a)
	192	(a)
316 Stainless steel	(a)	(a)

^aNo failure.

TABLE VI. - ROOM-TEMPERATURE TENSILE PROPERTIES^a OF TUBING
ALLOYS BEFORE AND AFTER ENDURANCE TESTING

Alloy	Rig environment	Rig exposure, hr	0.2-Percent-offset yield strength, MPa	Ultimate tensile strength, MPa	Elongation, percent
N-155	As received ^b	----	480	878	45
	Helium	1000	422	855	26
	Hydrogen	1000	455	834	16
A-286	As received ^b	----	364	699	34.5
	Helium	1000	378	724	14.5
	Hydrogen	1000	345	751	16.5
Incoloy 800	As received	----	293	600	38
	Helium	1000	235	616	26
	Hydrogen	1000	248	603	35
19-9DL	As received ^b	----	418	785	43
	Helium	520	289	717	46.5
	Hydrogen	820	341	678	31
Nitronic 40	As received	----	459	822	53
	Helium	532	407	797	51
	Hydrogen	619	414	797	42.5
316 Stainless steel	As received ^b	----	293	622	54
	Helium	1000	321	737	31
	Hydrogen	1000	294	703	31

^a Average of two tests except where noted.

^b Single test.

TABLE VII. - TENSILE PROPERTIES AT 760° C^a OF TUBING
ALLOYS BEFORE AND AFTER ENDURANCE TESTING

Alloy	Rig environment	Rig exposure, hr	0.2-Percent-offset yield strength, MPa	Ultimate tensile strength, MPa	Elongation, percent
N-155	As received	----	248	415	27
	Helium	1000	273	355	36
	Hydrogen	1000	262	375	34
A-286	As received	----	299	434	32
	Helium	1000	244	311	37.5
	Hydrogen	1000	234	302	36.5
Incoloy 800	As received	----	157	226	56
	Helium	1000	159	229	46
	Hydrogen	1000	142	231	55
19-9DL	As received	----	133	306	26.5
	Helium	520	159	228	43
	Hydrogen ^b	820	157	227	38
Nitronic 40	As received	----	181	286	29
	Helium	532	168	275	26
	Hydrogen ^b	619	168	272	24.5
316 Stainless steel	As received	----	128	226	50
	Helium	1000	152	242	42.5
	Hydrogen	1000	152	239	40.5

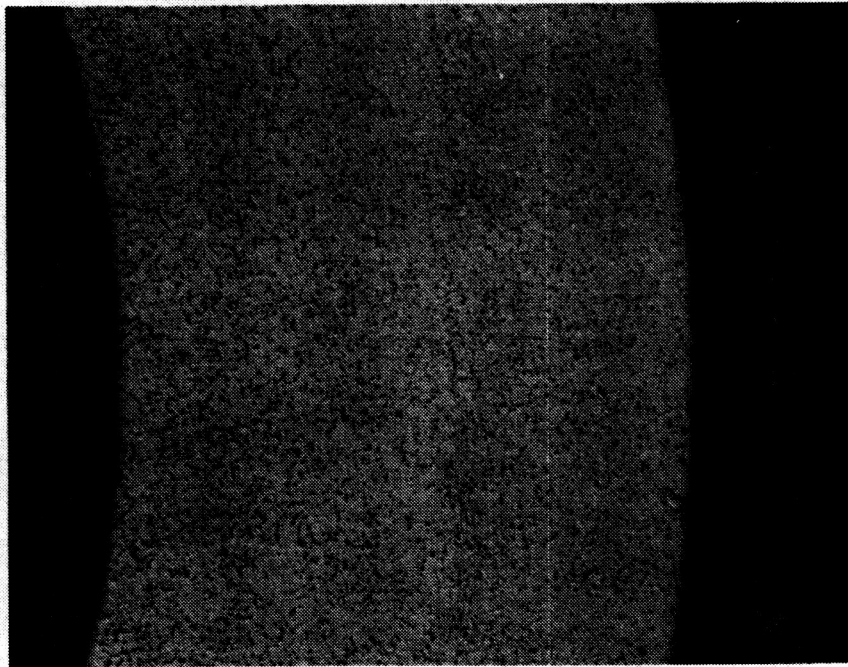
^aAverage of two tests except where noted.

^bSingle test.

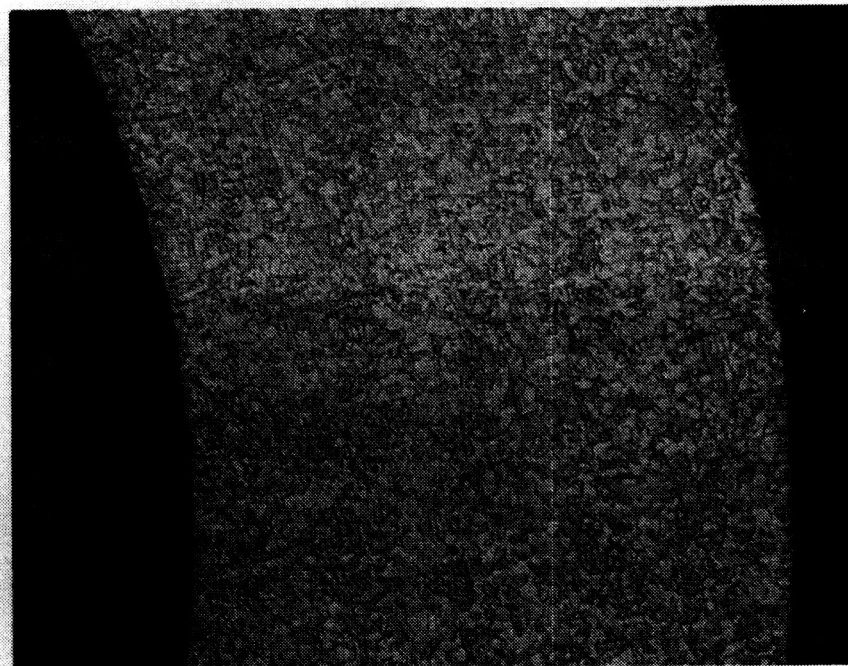
TABLE VIII. - AVERAGE AND PREDICTED
TUBING FAILURE TIMES AT 760° C

Alloy	Grain size, μm	Average failure time in helium, hr	Predicted life, ^a hr
N-155	17	>1000	60 000
A-286	11	855	2 400
Incoloy 800	32	807	2 000
19-9DL	9	232	500
Nitronic 40	15	154	375
316 Stainless steel	21	>1000	350

^aFrom ref. 7.



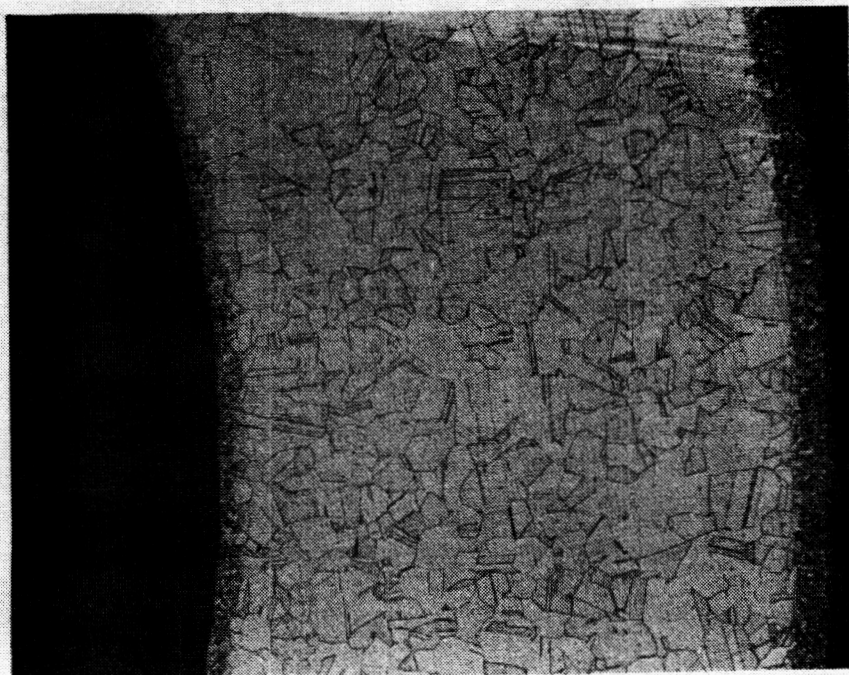
(a) N-155.



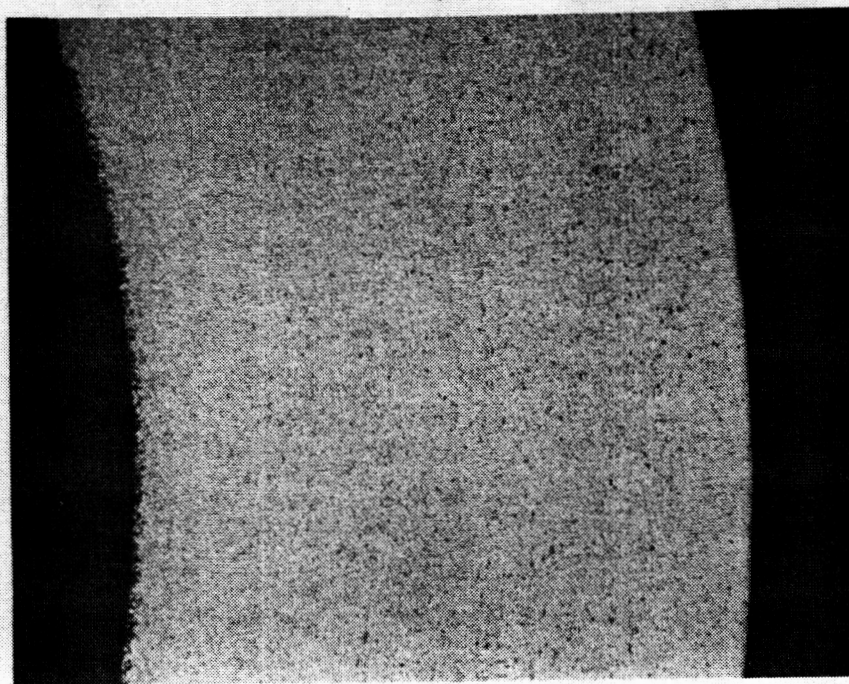
(b) A-286.

Figure 1. -Microstructures of as-recieved materials. Magnification, 100.

ORIGINAL PAGE IS
OF POOR QUALITY

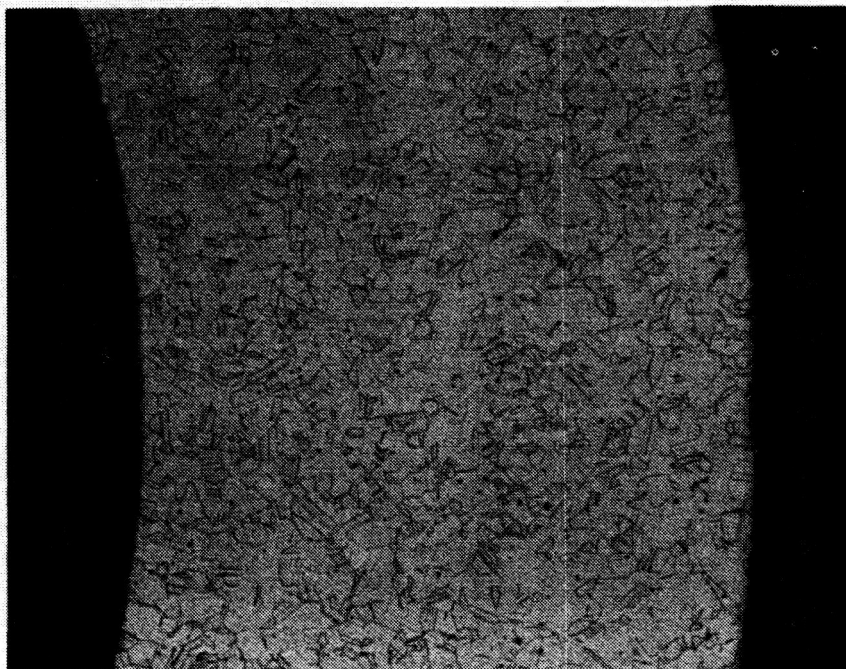


(c) Incoloy 800.

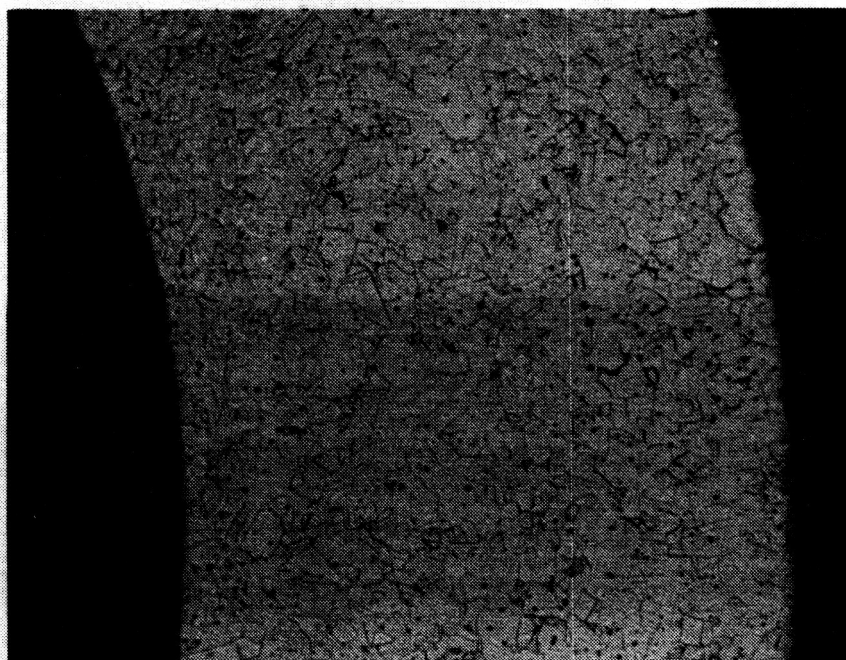


(d) 19-9DL

Figure 1. - Continued.



(e) Nitronic 40.



(f) 316 Stainless steel.

Figure 1. -Concluded.

ORIGINAL PAGE IS
OF POOR QUALITY

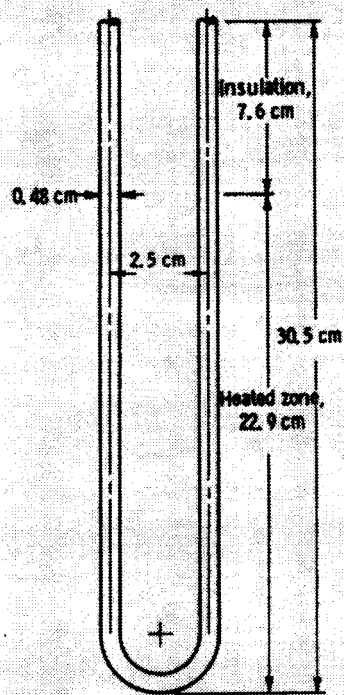


Figure 2. - Hairpin test specimen (not to scale).

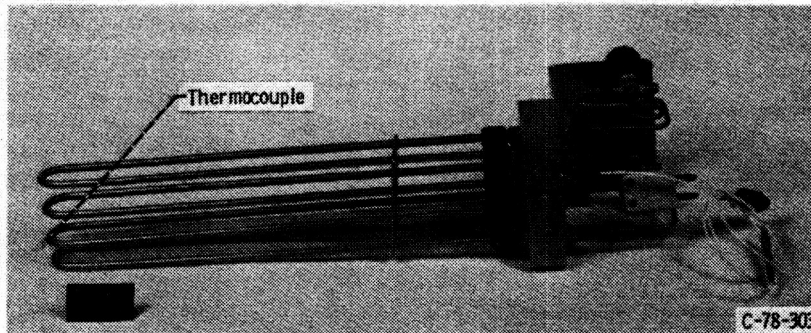


Figure 3. -Test module for Stirling engine simulator materials test rig.

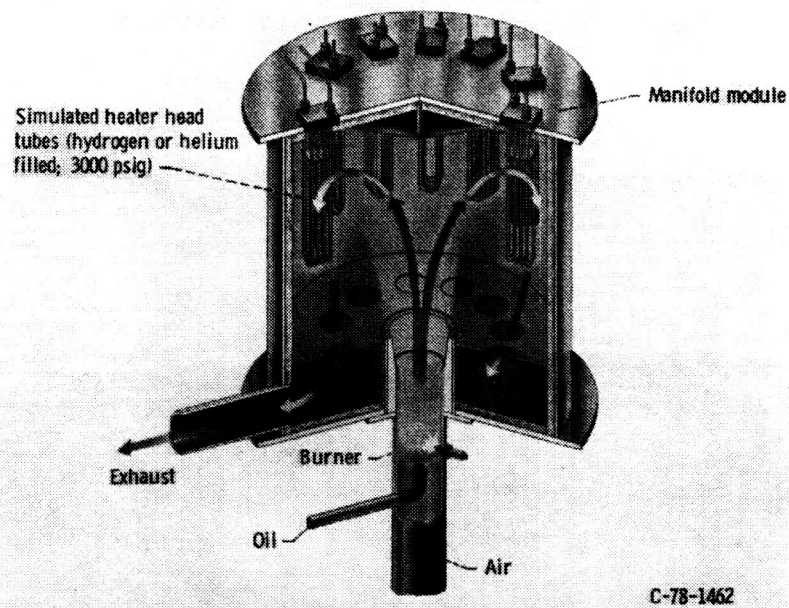


Figure 4. -Schematic representation of Stirling engine simulator materials test rig.

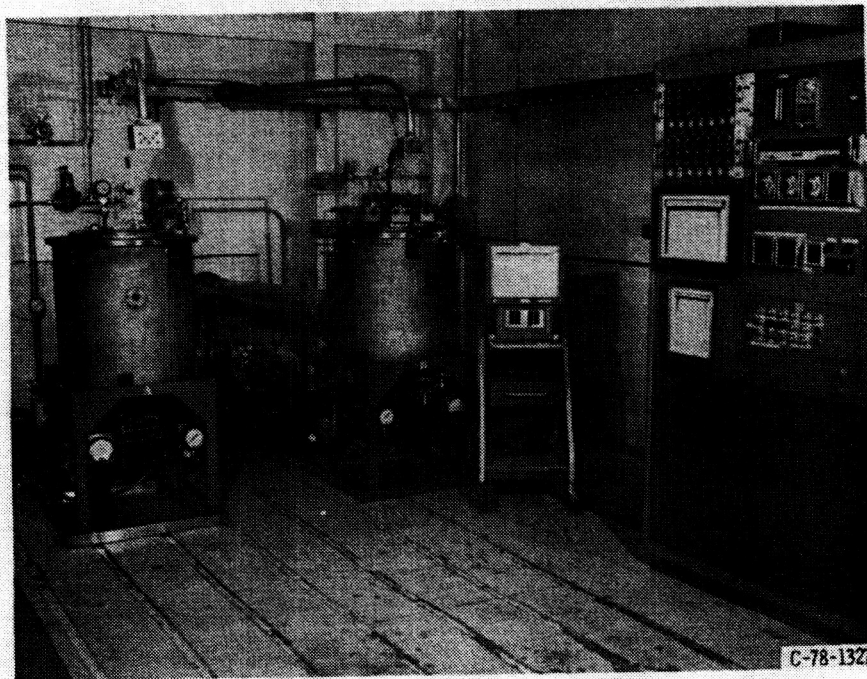


Figure 5. -Stirling engine simulator materials test rig, chambers A and B.

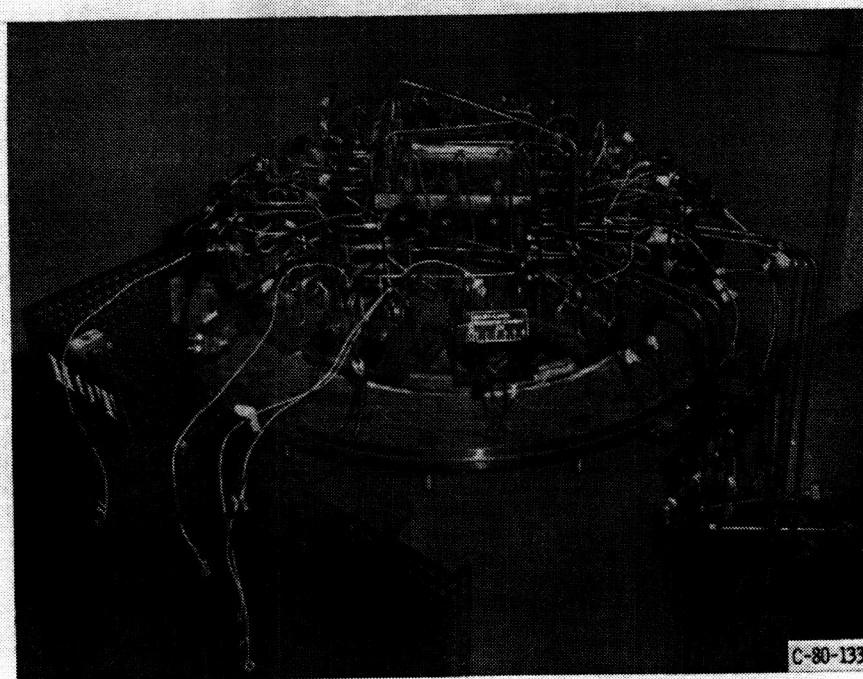


Figure 6. -Charging manifolds on Stirling simulator rig.

ORIGINAL PAGE IS
OF POOR QUALITY

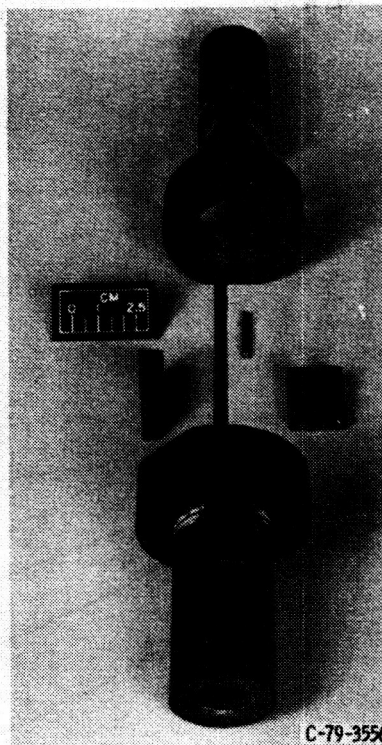


Figure 7. - Tube tensile specimen and grips.

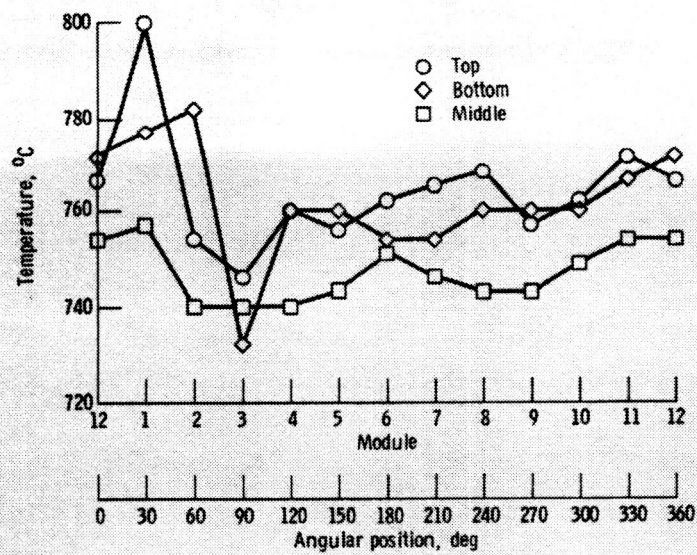


Figure 8. - Temperature profile in Stirling simulator rig.

ORIGINAL PAGE IS
POOR QUALITY

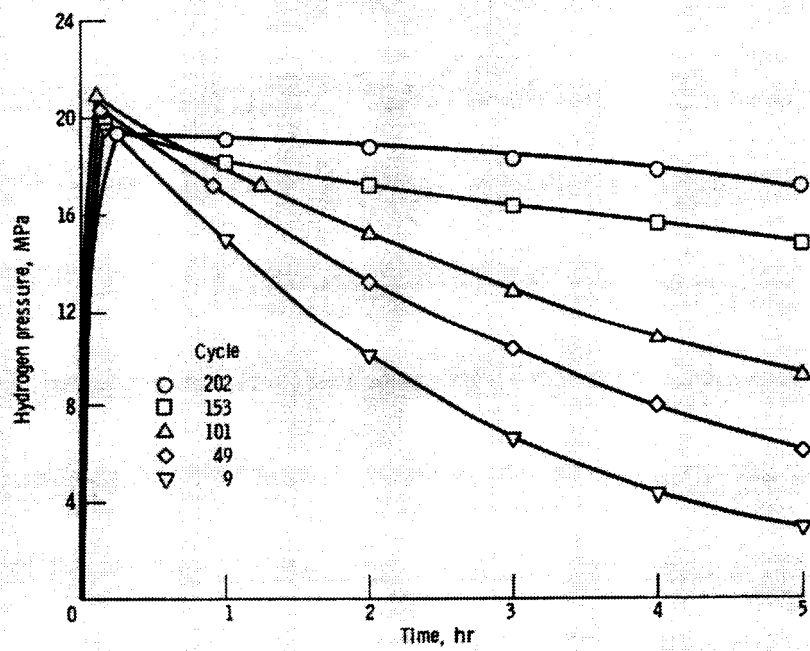
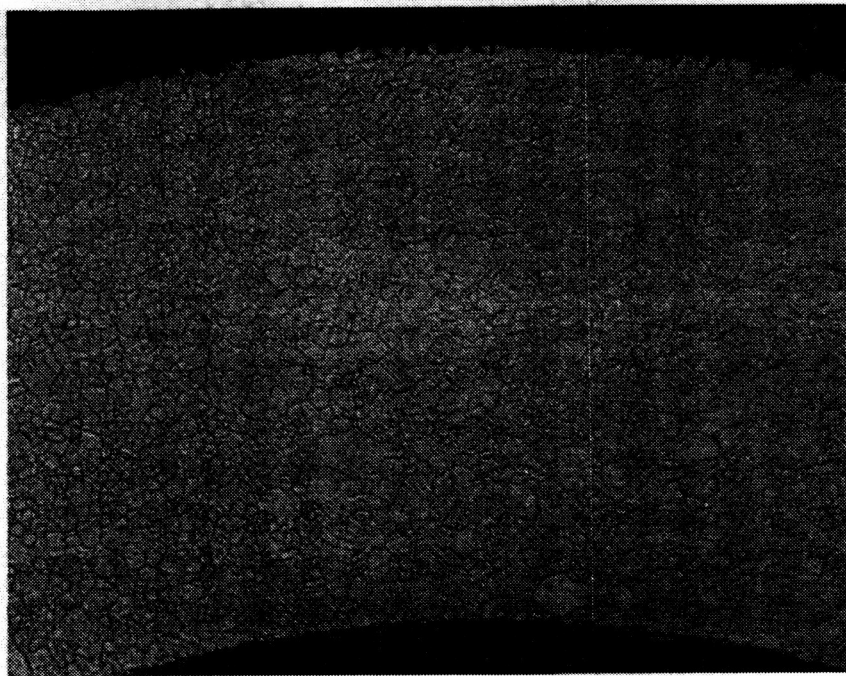
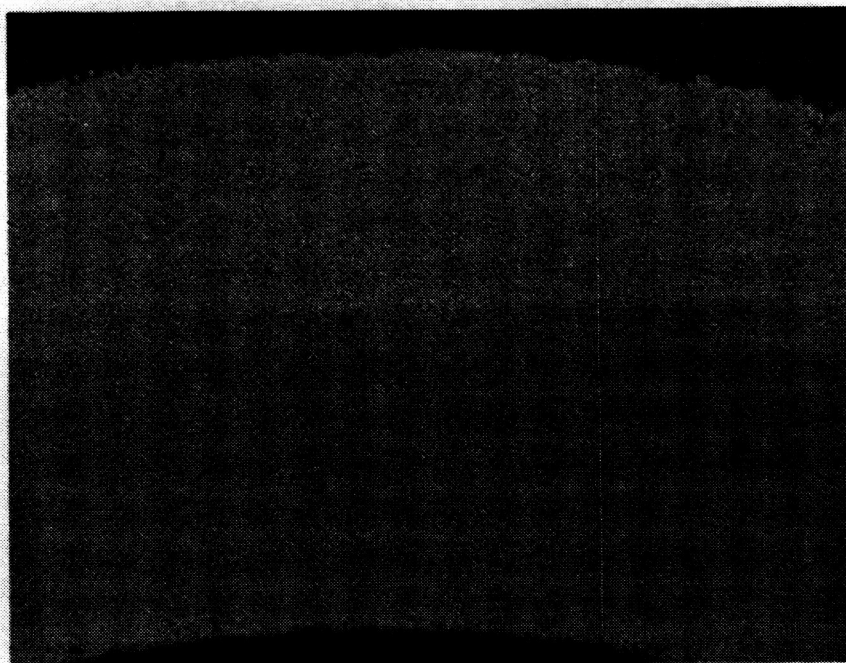


Figure 9. - Typical pressure decay curves for hydrogen-filled Incoloy 800 tubes.



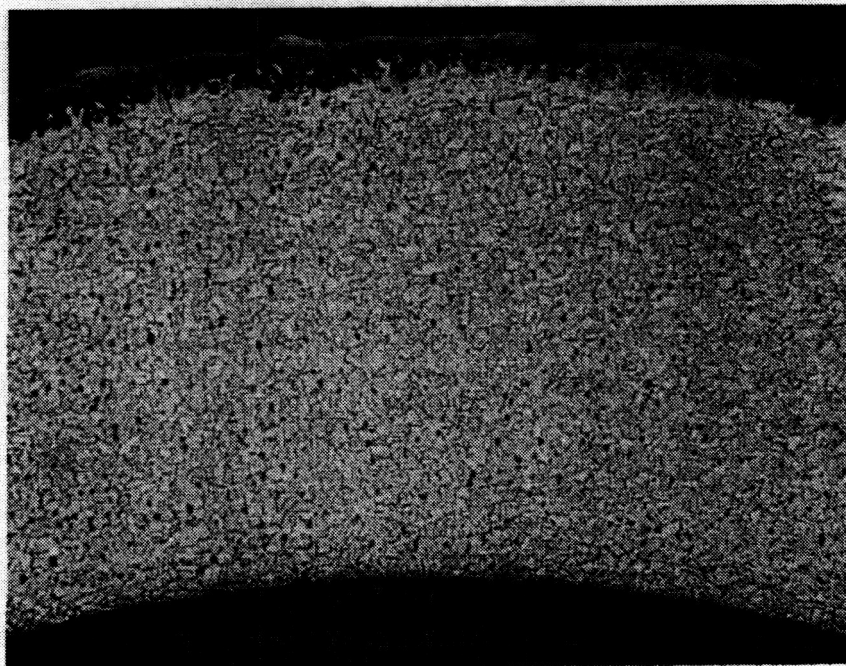
(a-1) 1000 Hours; helium filled.



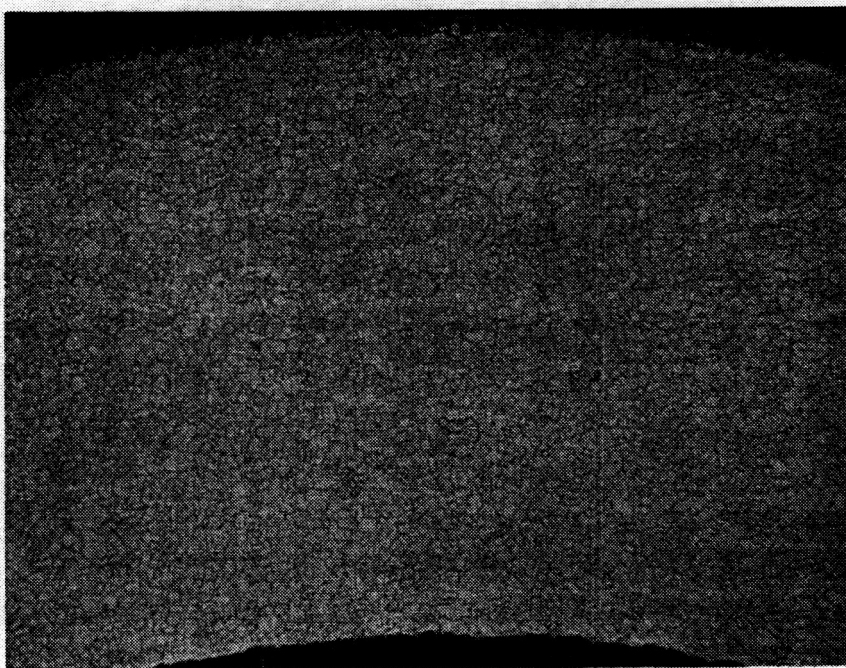
(a-2) 1000 Hours; hydrogen filled.

(a) N-155.

Figure 10. -Alloy microstructure after exposure in Stirling simulator rig. Magnification, 100.



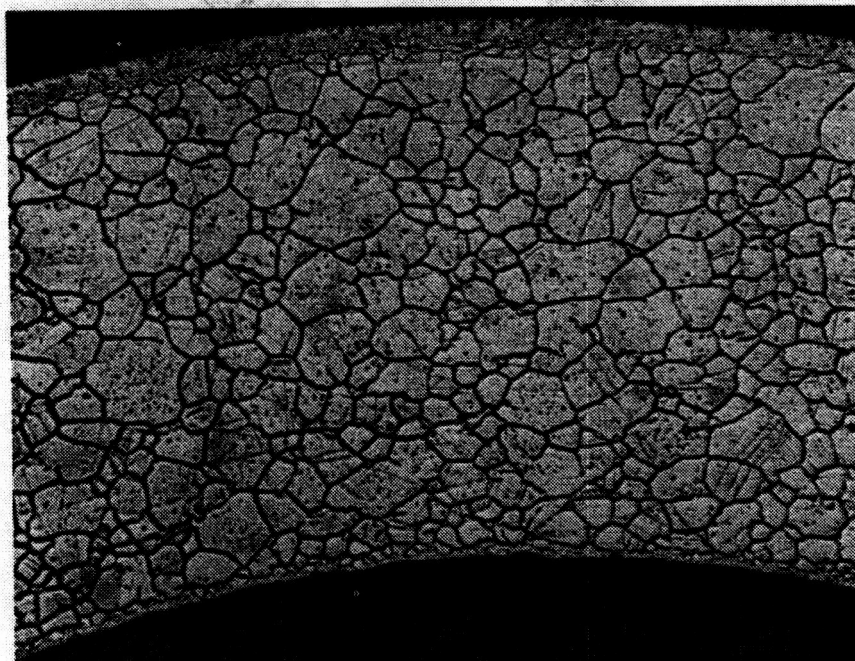
(b-1) 1000 Hours; helium filled.



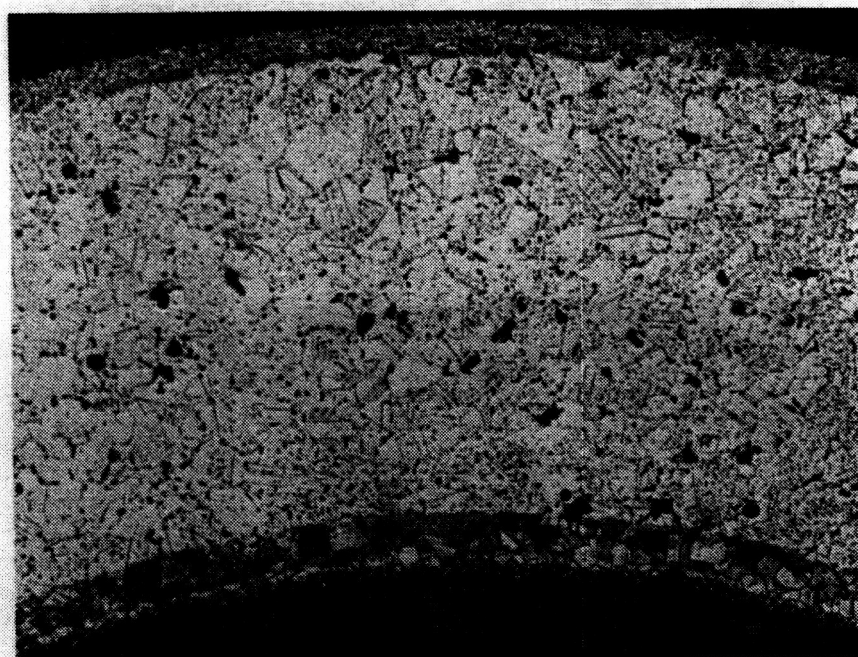
(b-2) 1000 Hours; hydrogen filled.

(b) A-286.

Figure 10. -Continued.



(c-1) 1000 Hours; helium filled.

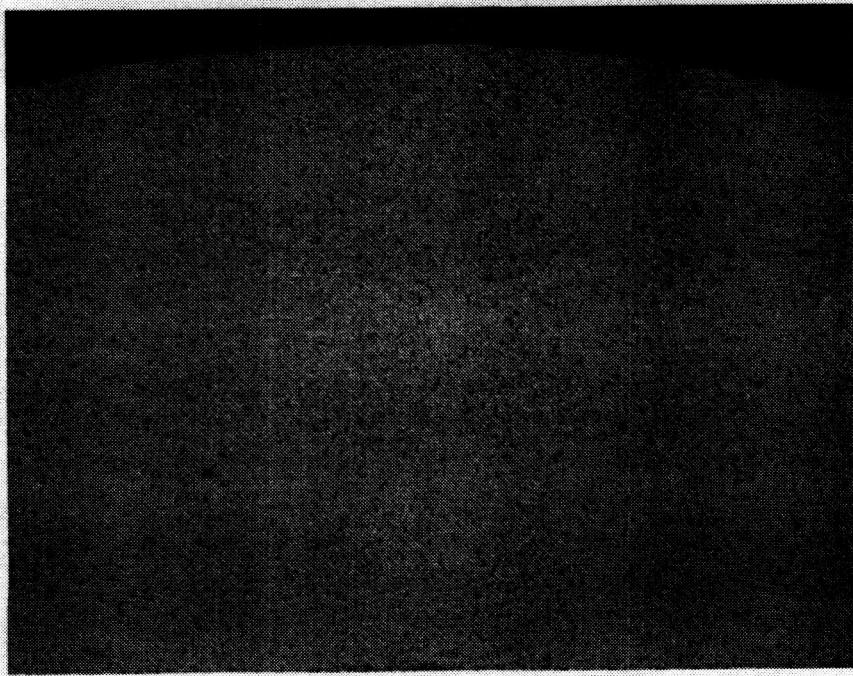


(c-2) 1000 Hours; hydrogen filled.

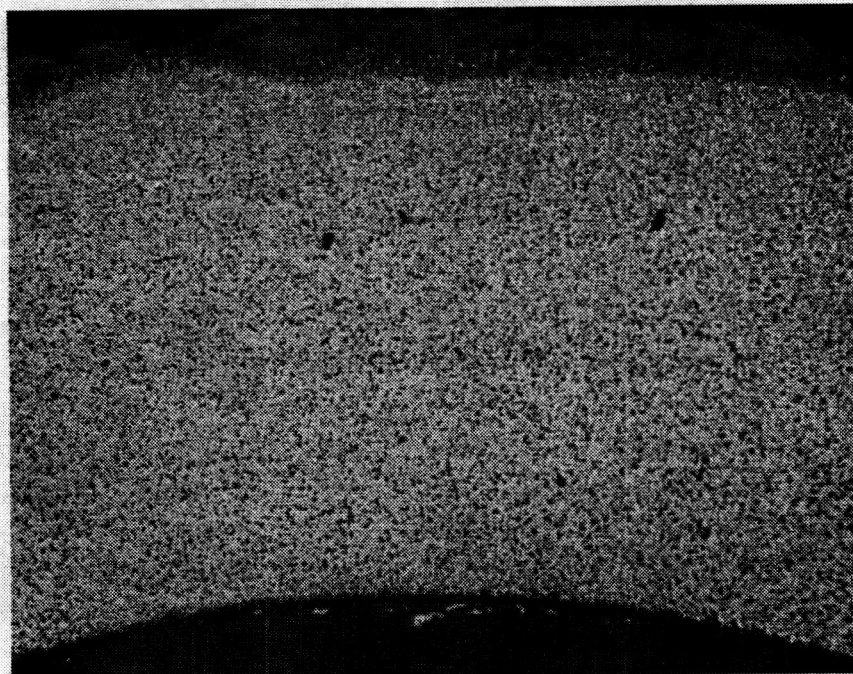
(c) Incoloy 800.

Figure 10. -Continued.

ORIGINAL PAGE IS
OF POOR QUALITY



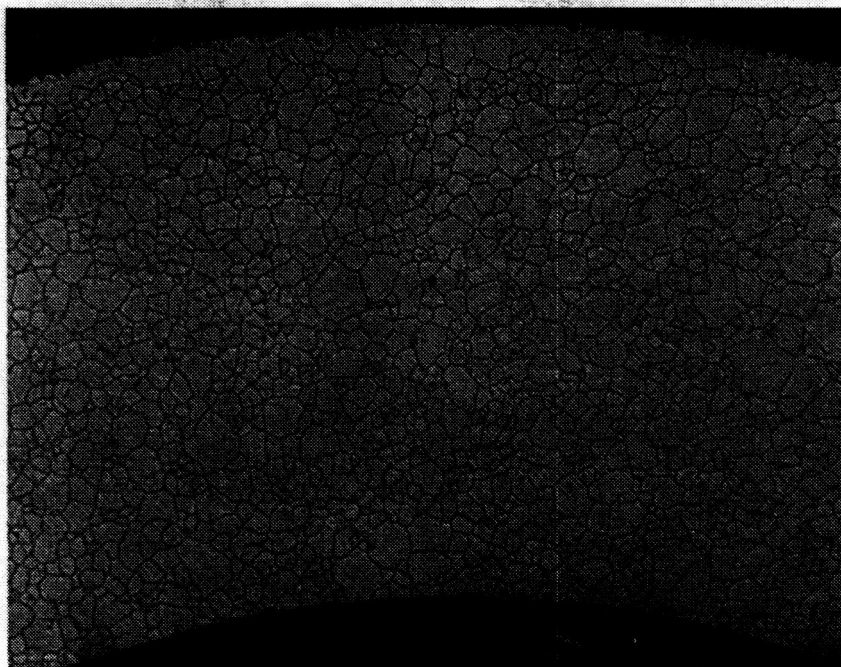
(d-1) 512 Hours; helium filled.



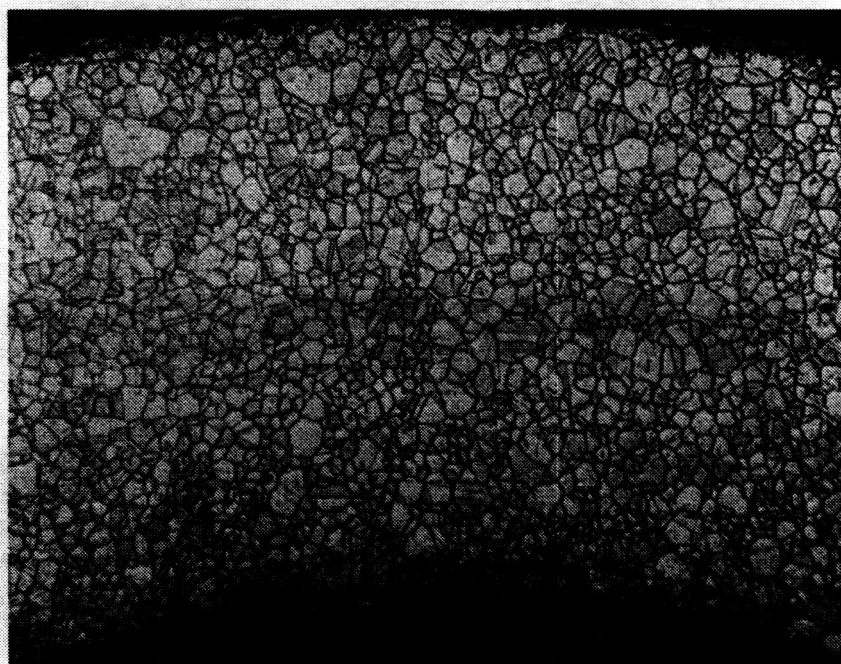
(d-2) 901 Hours; hydrogen filled.

(d) 19-9DL.

Figure 10. -Continued.



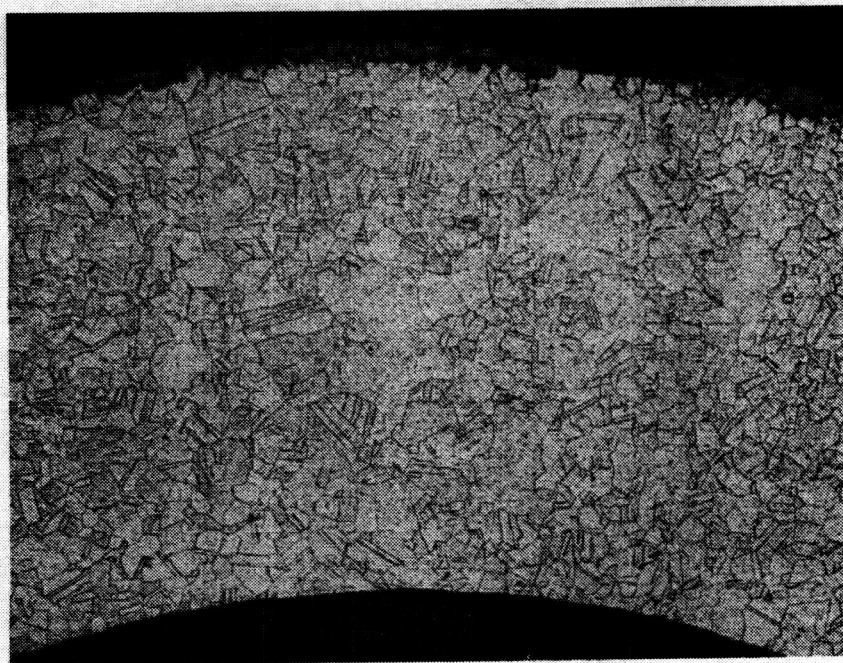
(e-1) 542 Hours; helium filled.



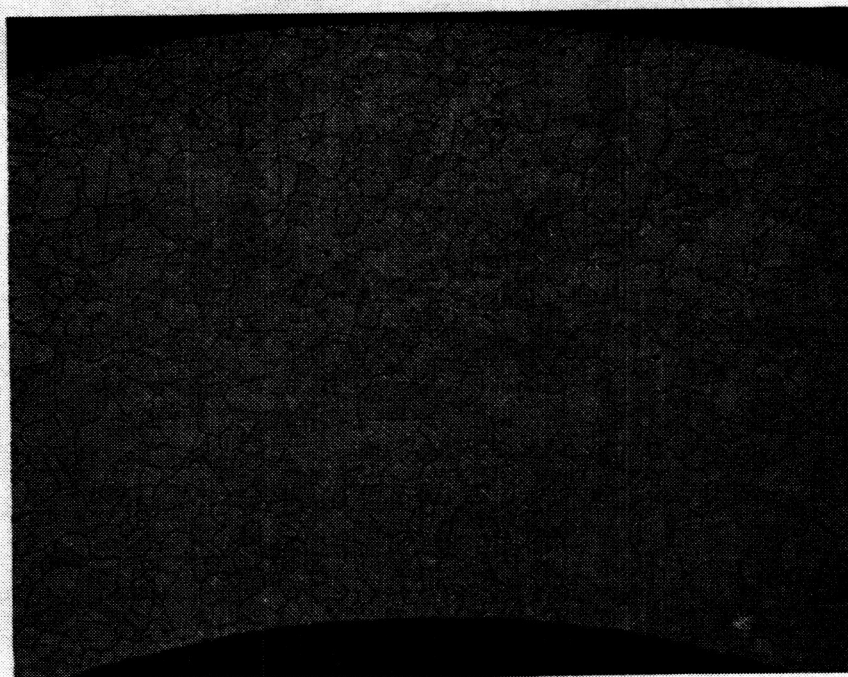
(e-2) 619 Hours; hydrogen filled.

(e) Nitronic 40.

Figure 10. -Continued.



(f-1) 1000 Hours; helium filled.



(f-2) 1000 Hours; hydrogen filled.

(f) 316 Stainless steel.

Figure 10. -Concluded.

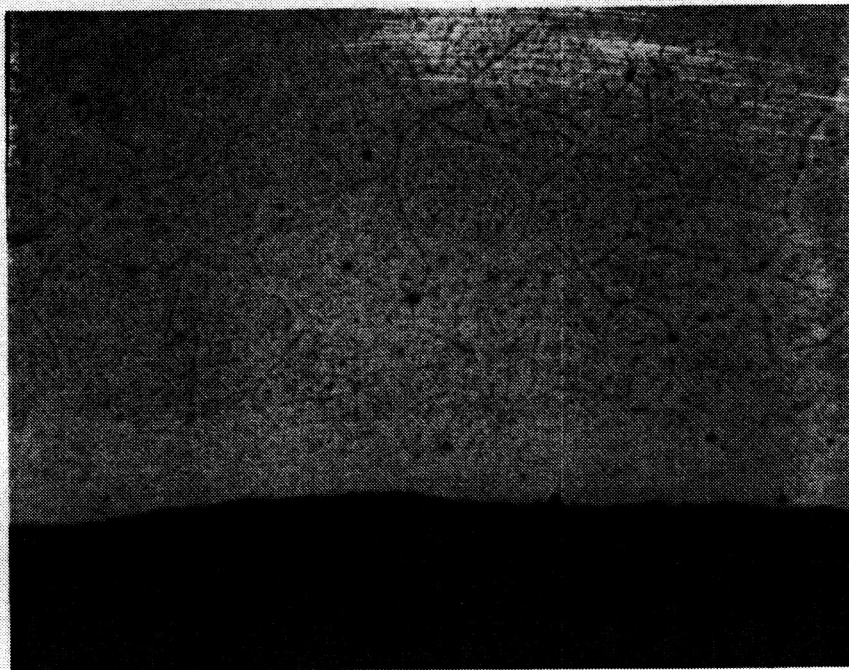
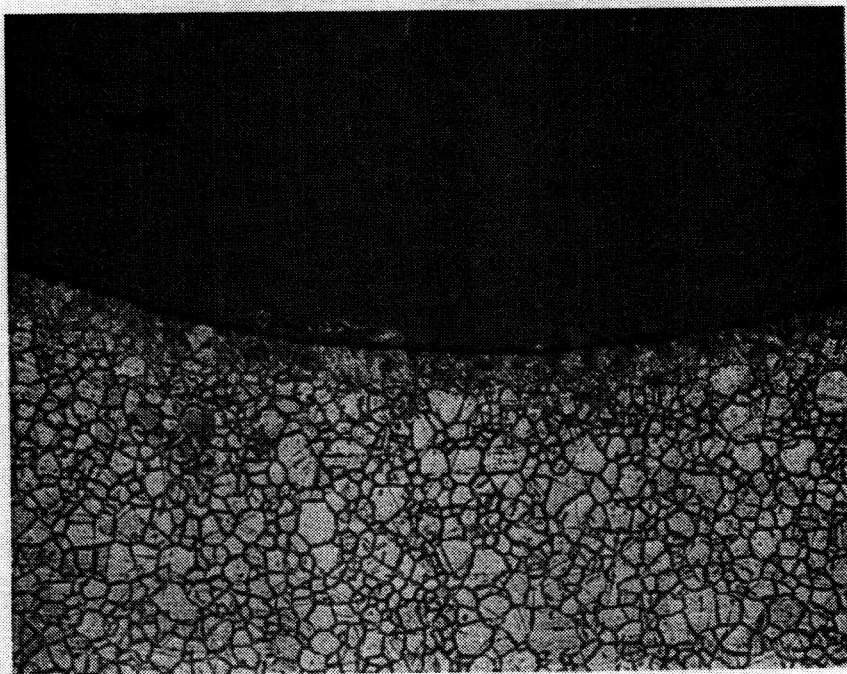


Figure 11. -Typical cross section of inner surface of hydrogen-filled tube after Stirling simulator rig exposure. Material, 316 stainless steel; magnification, 500.



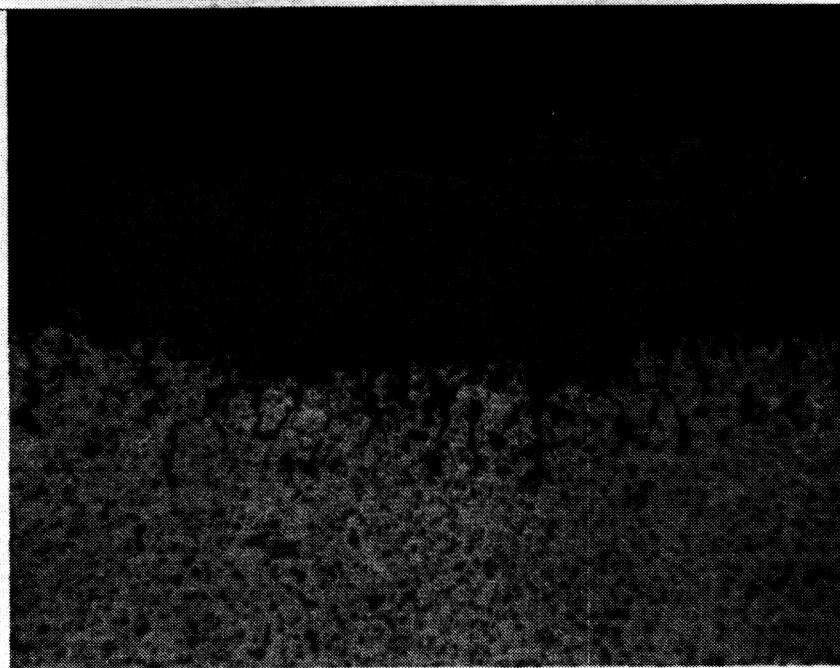
(a) Magnification, 100.



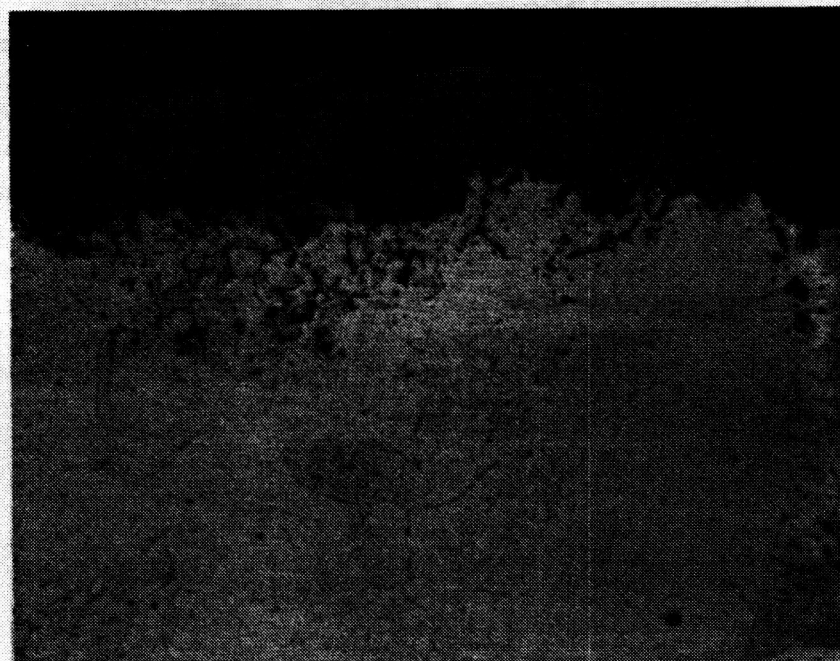
(b) Magnification, 500.

Figure 12. -Inner surface of hydrogen-filled Nitronic 40 tube after 619 hours in Stirling simulator rig.

ORIGINAL PAGE IS
OF POOR QUALITY



(a) 19-9DL



(b) 316 Stainless steel.

Figure 13. -Outer oxide scale formed on 19-9DL and 316 stainless steel during Stirling simulator rig exposure for 1000 hours at 760°C. Magnification, 500.